kcj

Korean Circulation Journal

Original Research

Check for updates

CircZNF609 Aggravated Myocardial Ischemia Reperfusion Injury via Mediation of miR-214-3p/PTGS2 Axis

Wen-Qiang Tang iD**, MM, Feng-Rui Yang** iD**, MD, Ke-Min Chen** iD**, MM, Huan Yang** iD**, MM, Yu Liu** iD**, MD, and Bo Dou** iD**, MM**

Department of Anesthesiology, The First Affiliated Hospital of University of South China, Hengyang, Hunan Province, P.R. China

Correspondence to
Bo Dou, MM
Department of Anesthesiology, The First Affiliated Hospital of University of South China, No.69, Chuanshan Road, Hengyang 421001, Hunan Province, P.R. China.
Email: bbnbboddrru789@163.com

ORCID iDs
Wen-Qiang Tang iD
https://orcid.org/0000-0002-8964-1490
Feng-Rui Yang iD
https://orcid.org/0000-0002-6767-6959
Ke-Min Chen iD
https://orcid.org/0000-0001-8350-1625
Huan Yang iD
https://orcid.org/0000-0002-9658-5378
Yu Liu iD
https://orcid.org/0000-0002-0248-688X
Bo Dou iD
https://orcid.org/0000-0003-0754-2083

AUTHOR'S SUMMARY

Circular RNAs were known to play vital role in myocardial ischemia reperfusion injury (MIRI), while the role of CircZNF609 in MIRI remains unclear. This study was aimed to investigate the function of CircZNF609 in MIRI. CircZNF609 aggravated the progression of MIRI via targeting miR-214-3p/PTGS2 axis, which suggested CircZNF609 might act as a vital modulator in MIRI.

ABSTRACT

Background and Objectives: Circular RNAs were known to play vital role in myocardial ischemia reperfusion injury (MIRI), while the role of CircZNF609 in MIRI remains unclear. This study was aimed to investigate the function of CircZNF609 in MIRI.
Methods: Hypoxia/reoxygenation (H/R) model was established to mimic MIRI *in vitro*. Quantitative polymerase chain reaction was performed to evaluate gene transcripts. Cellular localization of CircZNF609 and miR-214-3p were visualized by fluorescence in situ hybridization. Cell proliferation was determined by CCK-8. TUNEL assay and flow cytometry were applied to detect apoptosis. Lactate dehydrogenase was determined by commercial kit. ROS was detected by DCFH-DA probe. Direct interaction of indicated molecules was determined by RIP and dual luciferase assays. Western blot was used to quantify protein levels. *In vivo* model was established to further test the function of CircZNF609 in MIRI.
Results: CircZNF609 was upregulated in H/R model. Inhibition of CircZNF609 alleviated H/R induced apoptosis, ROS generation, restored cell proliferation in cardiomyocytes and human umbilical vein endothelial cells. Mechanically, CircZNF609 directly sponged miR-214-3p to release PTGS2 expression. Functional rescue experiments showed that miR-214-3p/PTGS2 axis was involved in the function of circZNG609 in H/R model. Furthermore, data in mouse model revealed that knockdown of CircZNF609 significantly reduced the area of myocardial infarction and decreased myocardial cell apoptosis.
Conclusions: CircZNF609 aggravated the progression of MIRI via targeting miR-214-3p/PTGS2 axis, which suggested CircZNF609 might act as a vital modulator in MIRI.

Keywords: PTGS2; Hypoxia; Ischemia reperfusion injury

Author Contributions
Conceptualization: Tang WQ; Data curation: Chen KM; Formal analysis: Yang H; Funding acquisition: Tang WQ; Investigation: Liu Y; Methodology: Yang H; Project administration: Dou B; Resources: Chen KM; Software: Liu Y; Supervision: Dou B; Validation: Dou B; Visualization: Liu Y; Writing - original draft: Yang FR; Writing - review & editing: Dou B.

INTRODUCTION

Acute myocardial infarction (AMI) results from the necrosis of cardiomyocytes, which is caused by coronary artery occlusion and insufficient blood supply. The incidence of AMI among people (<45 years old) has been increasing every year.[1] Myocardial ischemia/reperfusion injury (MIRI) refers to progressive aggravation of AMI, while the ischemic myocardium can be restored to normal perfusion after acute coronary artery occlusion.[2] The changes of myocardial ultrastructure, energy metabolism, cardiac function and electrophysiology caused by ischemia are more prominent after reperfusion. Although patients with AMI may receive timely reperfusion therapy, mortality rate of MIRI is still 10%.[3] Hence, it is urgent to investigate the pathogenesis of MIRI and explore novel therapeutic target for the treatment of MIRI.

Circular RNAs (circRNAs) were a class of non-coding RNA. Unlike linear RNA, circRNAs were enclosed in a circular structure and have higher RNA stability. Previous studies have revealed the function of circRNAs in MIRI. Zhou et al.[4] demonstrated that circRNA suppressed the progression of MIRI by inhibiting autophagy. Li et al.[5] illustrated that circular transcript of NCX1 gene was involved in the progress of MIRI through targeting miR-133; Song et al.[6] revealed that CircRNA TLK1 promoted the development MIRI via mediation of miR-214/RIPK1 axis. CircZNF609 was proved to participate in myogenesis.[7] Meanwhile, it was also reported that inhibition of CircZNF609 alleviated vascular endothelial dysfunction,[8] while the detailed function of CircZNF609 remains largely unknown.

Prostaglandin-endoperoxide synthase 2 (PTGS2), also named cyclooxygenase-2 (COX-2), was proved to be a critical mediator in inflammatory response.[9] It was well-known that AMI could upregulate the expression of PTGS2. Parecoxib, an inhibitor of PTGS2, was reported to inhibit the apoptosis during the progression of AMI.[10] In addition, it was reported that inhibition of COX-2 by sevoflurane showed beneficial effect on the progression of MIRI.[11] Moreover, lncRNA MALAT1 could exacerbate the inflammatory response via up-regulating PTGS2.[12] Hence, targeting PTGS2 might be an effective strategy for the treatment of MIRI.

In present study, our results revealed CircZNF609 was upregulated in MIRI, and knockdown of CircZNF609 could ameliorate the progression of MIRI. Mechanically, CircZNF609 reversed H/R-induced cell injury via binding with miR-214-3p, and functioned as a competing endogenous RNA (ceRNA) to upregulate PTGS2 expression. Our study might shed new insights on exploring the novel strategy against MIRI.

METHODS

Ethical statement
This article was approved by Institutional Animal Care and Use Committee (IACUC) of The First Affiliated Hospital of University of South China (20210309). This article does not contain any studies with human participants performed by any of the authors.

Cell culture and hypoxia/reoxygenation model
Human cardiomyocytes (HCMs) and human umbilical vein endothelial cells (HUVECs) were purchased from mingzhoubio (Ningbo, Zhejiang, China). The primary mouse cardiomyocytes were isolated from C57BL/6 mice following to previous described.[13] All cells

were cultured in DMEM (Invitrogen, Carlsbad, CA, USA). The medium was supplemented with 10% fetal bovine serum (FBS, Invitrogen), 100 U/mL penicillin, and 100 mg/mL streptomycin (Sigma, St. Louis, MA, USA) at 37°C with 5% CO_2. To construct the H/R model, cells were subjected to hypoxia in a hypoxic chamber (5% CO_2, 95% N_2, 37°C) for 16 h. Subsequently, the medium was replaced in the medium with DMEM with 10% FBS followed by 2 h of reoxygenation at 37°C with 5% CO_2.

Plasmid construction and transfection

si-NC, si-CircZNF609, si-PTGS2, NC mimic, NC inhibitor, miR-214 mimic, and miR-214-3p inhibitor were synthesized by GenePharma (Shanghai, China). Lipofectamine 3000 (Invitrogen) were used to perform the transfection according to the manufacturer's instruction. After 48 h, cells were treated by H/R stimulation or harvested for followed assays.

Cell counting kit-8

A total of $5×10^3$ cells were seeded on a 96-well plate incubated overnight. After that, adding 10 μL cell counting kit-8 (CCK-8) (Yeasen, Shanghai, China) reagent into per well and incubated the mixture for 2 h in dark. Absorbent values were measured at 450 nm by using a spectrophotometer (Bio-Rad, Hercules, CA, USA).

Detection of lactate dehydrogenase level

Cytotoxicity was detected by a lactate dehydrogenase (LDH) kit (Jiancheng, Jiangsu, China). The cell culture medium was obtained and centrifuged at 10,000×g for 15 min to collect supernatants. After incubation with reagents, the spectrophotometer (Bio-Rad) were applied to measure the OD value of each sample at 450 nm.

Reactive oxygen species

Fluorometric intracellular reactive oxygen species (ROS) kit (Sigma) with DCFH-DA was used for ROS detection. Treated HCM were washed with PBS. Test compounds (10 μM) were added into each group, and the cells was incubated for 1 h at 37°C with 5% CO_2. The fluorescence was measured at 520 nm by using a fluorescence microscope (Olympus, Nagoya, Japan).

Apoptosis assay

Annexin V-FITC/PI apoptosis detection kit (Invitrogen) was utilized for apoptotic test. After indicated treatment, cells were gathered and suspended with kit buffer, subsequently mixed with 0.5 μg/mL Annexin V-FITC and PI for 20 min at room temperature in the dark. After that, the percentage of apoptosis was acquired using a flow cytometer (Beckman Coulter Inc, Brea, CA, USA) and FlowJo VX10 Software (FlowJo LLC) was performed for numerical analysis.

TdT-mediated dUTP Nick-End Labeling (TUNEL)

TdT incubation buffer (Invitrogen) was prepared according to the instruction, after cells were stained with TdT incubation buffer for 1 h and DAPI for 5 min at 37°C in the dark, the liquid was removed, the percentage of apoptosis was calculated under a fluorescence microscope. Images were acquired at 460 nm for DAPI and 520 nm for FITC-12-dUT on a fluorescence microscope (Olympus).

In animal study, paraffin sections were washed, permeabilized, and then incubated with 50 μl TUNEL reaction mixtures in a wet box for 60 min at 37°C in the dark. For signal conversion, slides were incubated with 50 μL of peroxidase (POD) for 30 min at 37°C, rinsed with PBS, and

then incubated with 50 μL diaminobenzidine (DAB) substrate solution for 10 min at 25℃. Finally, the expression of apoptotic cells was observed under an optical microscope (Olympus).

Fluorescence in situ hybridization

RNA fluorescence in situ hybridization (FISH) was performed using specific probes to miR-214-3p and CircZNF609 sequence (Life Technologies). HCM cells were harvested when grown to 85% confluence, then fixation in 4% paraformaldehyde for 10 min. Hybridization buffer was prepared and added to each sample according to the manufacturers' instructions, the images were acquired with a fluorescence microscope (Olympus).

Dual-luciferase report assay

The Starbase 2.0 was performed to analyze the potential binding sites between two target gene. Wild-type (WT) or mutant type (MUT) of CircZNF609 or PTGS2 3'-UTR were cloned into the pmirGLO dual-luciferase reporter gene vector (Life Technologies), then recombinant vectors and miR-214-3p mimic or NC mimic were co-transfected with HCM cells for 24–48 h. After transfection, the luciferase activity was detected using a Dual-luciferase reporter assay system kit (Promega, Madison, WI, USA).

RNA immunoprecipitation

HCMs were transfected with miR-214-3p mimic and NC mimic, approximately $1×10^7$ cells were harvested and lysed in lysate supplemented with RNase inhibitor and proteinase inhibitor. AGO2 immunoprecipitation was performed with an AGO2-specific antibody (Abcam, Cambridge, UK). Cell extraction was mixed with RNA immunoprecipitation (RIP) buffer (Merck Millipore, Burlington, MA, USA) containing antibody-coupled sepharose beads coated with anti-AGO2 or anti-IgG antibody. After overnight incubation at 4℃, beads were washed with lysis buffer and the RNA was extracted using Trizol reagent (TaKaRa, Tokyo, Japan).

RNA isolation and quantitation polymerase chain reaction

Total RNA samples were extracted by RNA extraction reagent (Trizol reagent, TaKaRa) then 1 μg total RNA with RNase-free DNase system (TaKaRa) were obtained for cDNA synthesis by using the reverse transcription kit (RiboBio, Guangzhou, China). For quantitative real-time polymerase chain reaction, 1 μg cDNA template was amplified by SYBR Premix kit (TaKaRa) on an ABI 7500 sequence detection system. The primers used in the reaction were listed as **Table 1**. β-actin and U6 served as the internal references. The $2^{-\Delta\Delta Ct}$ method was used to evaluate the relative fold changes. Each experiment was performed in triplicate.

Table 1. The primer sequences in this experiments

Gene	Forward/Reverse	Primer sequences (5'-3')
CircZNF609 (Human)	Forward	CAGCGCTCAATCCTTTGGGA
	Reverse	GACCTGCCACATTGGTCAGTA
miR-214-3p (Human)	Forward	GTGCAGGGTCCGAGGT
	Reverse	ATCATAGAGGAAAATCCACG
PTGS2 (Human)	Forward	TGTATCCTCCCACTGTCA
	Reverse	GATTAGCCT GCTTGTCTG
U6 (Human)	Forward	CTCGCTTCGGCAGCACA
	Reverse	AACGCTTCACGAATTTGCGT
β-actin (Human)	Forward	GGCACCACACCTTCTACAAT
	Reverse	GTGGTGGTGAAGCTGTAGCC

Western blot

The myocardial tissue and cells were lysed in RIPA lysis reagent, then the lysates were centrifuged at 10,000×g for 15 min. Protein concentration was determined by BCA protein assay kit (Dingguo, Beijing, China). Total protein was separated in 10% SDS-PAGE and transferred to PVDF membranes. After blocking with 5% nonfat milk, the membranes were incubated with the specific primary antibodies includinganti-Bcl-2 (ab182858, 1:2,000, Abcam), anti-Bax (ab32503, 1:1,000, Abcam), anti-caspase-3 (ab184787, 1:2,000, Abcam), anti-PTGS2 (ab179800, 1:2,000, Abcam) and β-actin (ab8226, 1:1,000, Abcam) diluted in blocking buffer at 4°C overnight, then the membranes were incubated with HRP-conjugated secondary antibodies (ab288151, 1:5,000, Abcam) at room temperature for 1 h. The signals were visualized by an enhanced ECL kit (Yeasen) and quantified by Image J software.

In vivo experiment

Male C57BL/6 mice (n=20, weighing 25–27 g) were purchased from the laboratory animal center of Zhengzhou University, and kept in the cages with 12 h light/dark cycle under controlled temperature of 25°C with free access to food and water. All animal experiments were approved by Institutional Animal Care and Use Committee (IACUC) of The First Affiliated Hospital of University of South China.

All Mice were randomly divided into four group: sham, model, Model + si-NC, model+si-circZNF609 (n=5 per group). The mice were first anesthetized with 40 mg/kg of sodium pentobarbital (Sigma) via intraperitoneal injection and were subjected to AMI by ligation of the left anterior descending (LAD) coronary artery.[14] Lentivirus packaged si-CircZNF609 or si-NC were acquired from Genepharma. To explore the effect of CircZNF609 silence on heart function, 200 μL si-CircZNF609 or si-NC ($5×10^9$/100 μL) were injected into apex of heart of mice after LAD ligation for 7 days. Heart tissues were collected for subsequent analysis. All the mice were followed up 4 weeks after MI induction. Finally, mice were sacrificed for collection of tissues.

Statistical analysis

All data were obtained from at least three independent experiments and analyzed by GraphPad Prism version 7.0. Comparison was performed by t-test or one-way ANOVA analysis. P<0.05 was considered statistically significance.

RESULTS

CircZNF609 was upregulated in hypoxia/reoxygenation -induced human cardiomyocytes

Firstly, HCMs were exposed to the condition of H/R. The data revealed that the expression of CircZNF609 was remarkably elevated in H/R group (1.00±0.19 vs. 1.93±0.25, p=0.007) (**Figure 1A**), and CircZNF609 was mainly distributed in cytoplasm of HCMs (cytoplasm, 0.68±0.09; nuclear 0.32±0.07) (**Figure 1B**). These results were also supported by FISH assay, as the green fluorescence was observed in cytosol and nucleus, especially in cytosol (**Figure 1C**). Collectively, these results indicated that CircZNF609 was upregulated in H/R model and mainly distributed in cytosol of HCMs.
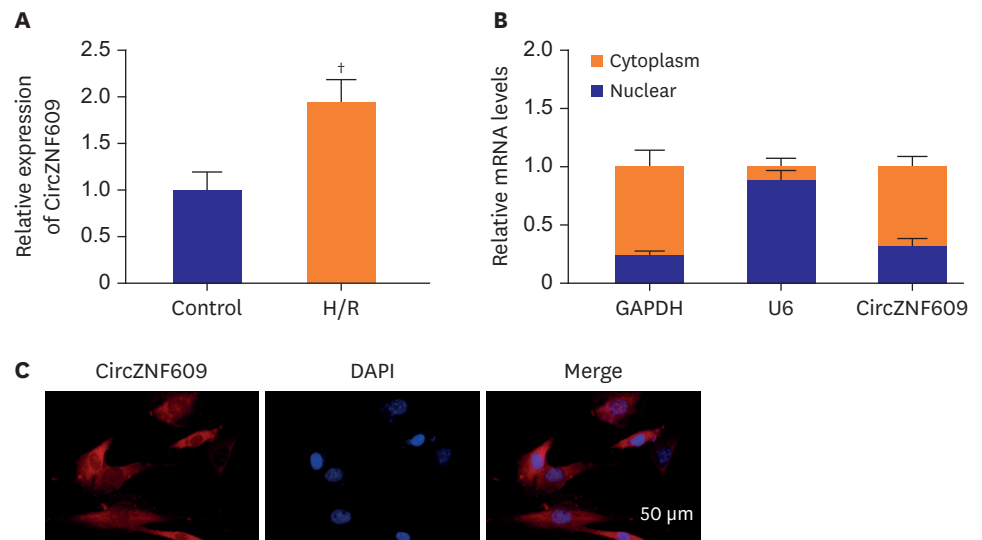
Figure 1. CircZNF609 was upregulated in H/R model. (A) Human cardiomyocytes were subjected to H/R model as aforementioned. qPCR was performed to detect the expression of CircZNF609. (B) Expression of CircZNF609 in nucleus and cytosol were determined by qPCR. (C) Subcellular location of CircZNF609 was observed by fluorescence in situ hybridization (n=3).

H/R = hypoxia/reoxygenation; qPCR = quantitative polymerase chain reaction.

*p<0.05; †p<0.01; ‡p<0.001.

Knockdown of CircZNF609 ameliorated H/R induced HCM damage

To investigate the functional significance of CircZNF609 in vitro, we used siRNA to knockdown CircZNF609 in HCMs before H/R stimulation. Quantitative polymerase chain reaction (qPCR) showed that comparted to si-NC (negative control siRNA) group, the expression of CircZNF609 in si-CircZNF609 group was substantially decreased, indicating successful knockdown of CircZNF609 in HCMs (1.00±0.11 vs. 0.45±0.07, p=0.002) (**Figure 2A**). It was showed that the proliferation of HCMs were notably impaired by H/R stimulation (100.00±8.15% vs. 57.49±13.08%, p=0.009), while knockdown of CircZNF609 significantly restored the cell proliferation (49.60±5.14% vs. 83.71±9.85%, p=0.006) (**Figure 2B**). The cell cytotoxicity indicated by LDH releasing was observed upon H/R stimulation (1.00±0.10 vs. 2.34±0.13, p=0.000), however, CircZNF609 knockdown attenuated the cytotoxicity (2.28±0.24 vs. 1.44±0.18, p=0.008) (**Figure 2C**). ROS generation was also substantially elevated upon H/R stimulation whereas CircZNF609 knockdown inhibited the generation of ROS (**Figure 2D**). Moreover, flow cytometry and TUNEL assay showed that H/R treatment triggered cell apoptosis (6.52±1.80% vs. 33.60±1.63%, p=0.000), whereas knockdown of CircZNF609 significantly compromised H/R induced apoptosis (36.18±3.06% vs. 18.08±3.63%, p=0.003) (**Figure 2E and F**). Additionally, results of western blots suggested that H/R induced expression of Bax (0.30±0.09 vs. 0.70±0.06, p=0.004), cleaved caspase 3 (0.18±0.05 vs. 0.65±0.11, p=0.003) and repressed the expression of Bcl-2 (0.72±0.06 vs. 0.32±0.12, p=0.007), however, CircZNF609 inhibition partially reversed the expression patterns induced by H/R stimulation (Bcl-2, 0.37±0.05 vs. 0.72±0.07, p=0.002; Bax, 0.81±0.06 vs. 0.52±0.10, p=0.011; cleaved-caspase 3, 0.66±0.60 vs. 0.33±0.05, p=0.002) (**Figure 2G**). Taken together, the above findings revealed that CircZNF609 knockdown ameliorated H/R induced injury in HCMs.

CircZNF609 sponged miR-214-3p

We next investigate the downstream molecule regulated by CircZNF609. Starbase 2.0 (http://starbase.sysu.edu.cn/) was used to predict the possible downstream target miRNAs of circZNF609. Among of them, we screened 5 target miRNAs that play a protective role in
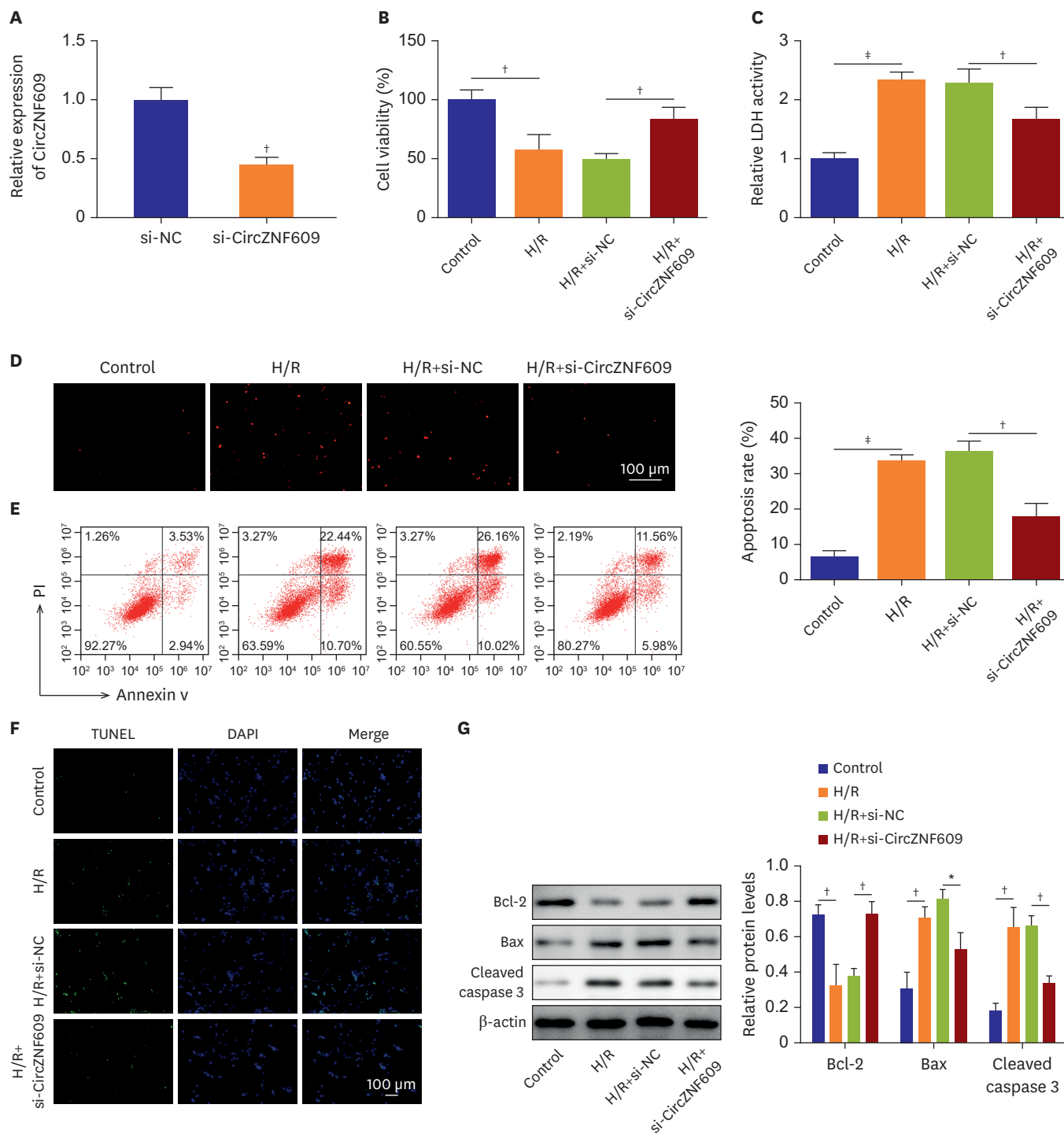
Figure 2. Knockdown of CircZNF609 ameliorated H/R induced myocardial injury. siRNA was transfected to HCMs to knockdown CircZNF609 in HCMs before H/R stimulation. (A) Expression of CircZNF609 was determined by qPCR. (B) Cell proliferation was evaluated by CCK-8 assay. (C) Cytotoxicity was evaluated by LDH assay. (D) ROS generation was detected by a ROS kit. (E) Cell apoptosis was determined by flow cytometry. (F) Cell apoptosis was determined by TUNEL. (G) Protein level of Bcl-2, Bax, cleaved caspase 3 were evaluated by western blots (n=3).
HCM = human cardiomyocyte; H/R = hypoxia/reoxygenation; LDH = lactate dehydrogenase; ROS = reactive oxygen species.
*p<0.05; †p<0.01; ‡p<0.001.

AMI, including miR-483-3p,[15] miR-378a-3p,[16] miR-204-5p,[17] miR-136-5p,[18] miR-214-3p.[6] The molecular connections and expression regulations between miRNAs and circZNF609 were validated utilizing qPCR and dual luciferase assay (**Supplementary Figure 1**), showing that circZNF609 could directly sponged these miRNAs (miR-483-3p, 1.00±0.08 vs. 0.75±0.09, p=0.022; miR-378a-3p, 1.00±0.11 vs. 0.77±0.08, p=0.047; miR-204-5p, 1.00±0.16 vs. 0.52±0.11, p=0.014; miR-136-5p, 1.00±0.05 vs. 0.69±0.07, p=0.003; miR-214-3p, 1.00±0.07 vs. 0.50±0.14, p=0.006), and negatively regulated them expressions to varying degrees (miR-483-3p, 1.00±0.11 vs. 1.46±0.18, p=0.020; miR-378a-3p, 1.00±0.15 vs. 1.66±0.10, p=0.003; miR-204-5p, 1.00±0.10 vs. 1.00±0.10, p=0.002; miR-136-5p, 1.00±0.14 vs. 1.62±0.12, p=0.005; miR-214-3p, 1.00±0.16 vs. 1.78±0.11, p=0.002). Thus, miR-214-3p was enrolled for next investigation. Starbase 2.0 was used to predict potential binding site between miR-214-3p and CircZNF609 (**Figure 3A**). It was well-known that miRNAs exerted function by binding with AGO2. RIP assay showed that CircZNF609 was enriched in the AGO2 protein immunoprecipitates (1.00±0.22 vs. 4.22±0.46, p=0.000) (**Figure 3B**). Moreover, results showed that when co-transfected with WT-binding sequence, miR-214-3p mimics substantially repressed relative luciferase activity (1.00±0.07 vs. 0.50±0.14, p=0.006). However, miR-214-3p didn't show significant influence on relative luciferase activity when co-transfected with MUT-binding sequence (1.00±0.11 vs. 0.92±0.06, p=0.345) (**Figure 3C**). Moreover, FISH assay revealed that CircZNF609 was co-localized with miR-214-3p in the cytosol of HCMs (**Figure 3D**). Interestingly, we also observed that inhibition of CircZNF609 led an increase of miR-214-3p (1.00±0.16 vs. 1.78±0.11, p=0.002) (**Figure 3E**). Collectively, these results indicated that CircZNF609 directly bound with miR-214-3p.

MiR-214-3p targeted PTGS2

Similarly, the potential targets miR-214-3p was predicted using Starbase 2.0 (http://starbase. sysu.edu.cn/). Combining literature screening, NLRC5,[19] PTGS2,[12] Bax,[20] MAPK1[21] and PTEN[22] were selected into our detections duo to their roles in AMI. Dual luciferase assay validated the
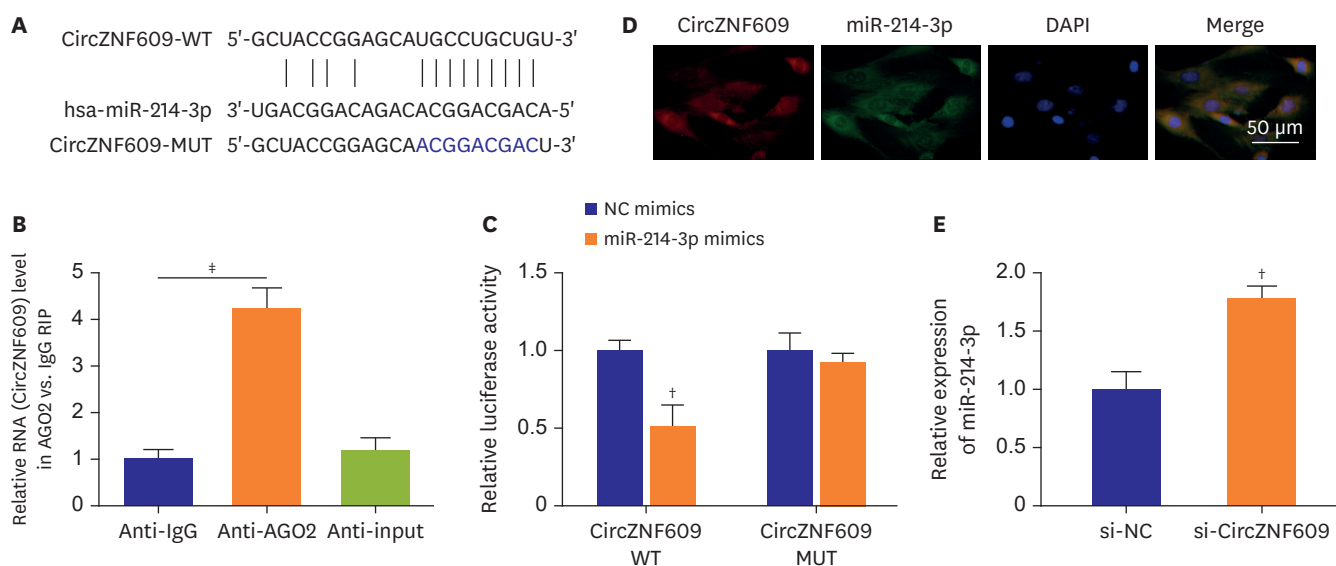

Figure 3. CircZNF609 functioned as a sponge of miR-214-3p. (A) Starbase 2.0 was used to predict the potential binding site of miR-214-3p and CircZNF609. (B) RNA immunoprecipitation was performed in HCMs to evaluate the enrichment of CircZNF609 in AGO2-pulled complex. (C) Direct binding of miR-214-3p and CircZNF609 was verified by dual luciferase assay. (D) Subcellular location of CircZNF609 and miR-214-3p in HCMs was observed by FISH. (E) Expression of miR-214-3p was determined by quantitative polymerase chain reaction (n=3).
HCM = human cardiomyocyte; MUT = mutant type; WT = wild-type.
*p<0.05; †p<0.01; ‡p<0.001.

direct targeting relationship between these mRNAs and miR-214-3p (NLRC5, 1.00±0.09 vs. 0.75±0.07, p=0.019; PTGS2, 1.00±0.17 vs. 0.60±0.11, p=0.029; Bax, 1.00±0.08 vs. 0.68±0.09, p=0.010; MAPK1, 1.00±0.14 vs. 0.54±0.11, p=0.011; PTEN, 0.54±0.11 vs. 0.45±0.13, p=0.004) (**Supplementary Figure 2A and B**). In addition, qPCR analysis also indicated that miR-214-3p negatively regulated the mRNA expressions in cardiomyocytes (NLRC5, 1.00±0.19 vs. 1.00±0.21, p=0.011, 1.00±0.21 vs. 2.41±0.20, p=0.002; PTGS2, 1.00±0.21 vs. 0.33±0.12, p=0.010, 1.02±0.16 vs. 2.32±0.27, p=0.002; Bax, 1.00±0.20 vs. 0.44±0.09, p=0.011, 0.97±0.17 vs. 1.77±0.10, p=0.002; MAPK1, 1.00±0.12 vs. 0.45±0.16, p=0.009, 1.15±0.27 vs. 2.36±0.22, p=0.004; PTEN, 1.00±0.19 vs. 0.33±0.13, p=0.018, 1.03±0.16 vs. 2.90±0.36, p=0.007) (**Supplementary Figure 2C**). Afterwards, the MUT/WT-luciferase sequences were constructed as shown in **Figure 4A**. Results showed that when co-transfected with WT-binding sequence, miR-214-3p mimic substantially suppressed relative luciferase activity (1.00±0.17 vs. 0.60±0.11, p=0.029). However, miR-214-3p didn't show significant influence on relative luciferase activity when co-transfected with mutant binding sequence (1.00±0.10 vs. 1.03±0.08, p=0.700) (**Figure 4B**). Moreover, we also found that mRNA and protein expression of PTGS2 were suppressed by miR-214-3p mimics (mRNA, 1.00±0.21 vs. 0.33±0.12, p=0.001; Protein, 0.39±0.04 vs. 0.22±0.06, p<0.018) and elevated by miR-214-3p inhibitor (mRNA, 1.02±0.16 vs. 2.32±0.27, p=0.002; Protein, 0.37±0.06 vs. 0.64±0.08, p=0.009) indicated by the results of qPCR and western blots (**Figure 4D**). Taken together, results in this section suggested that miR-214-3p directly targeted PTGS2 and negatively regulated PTGS2.
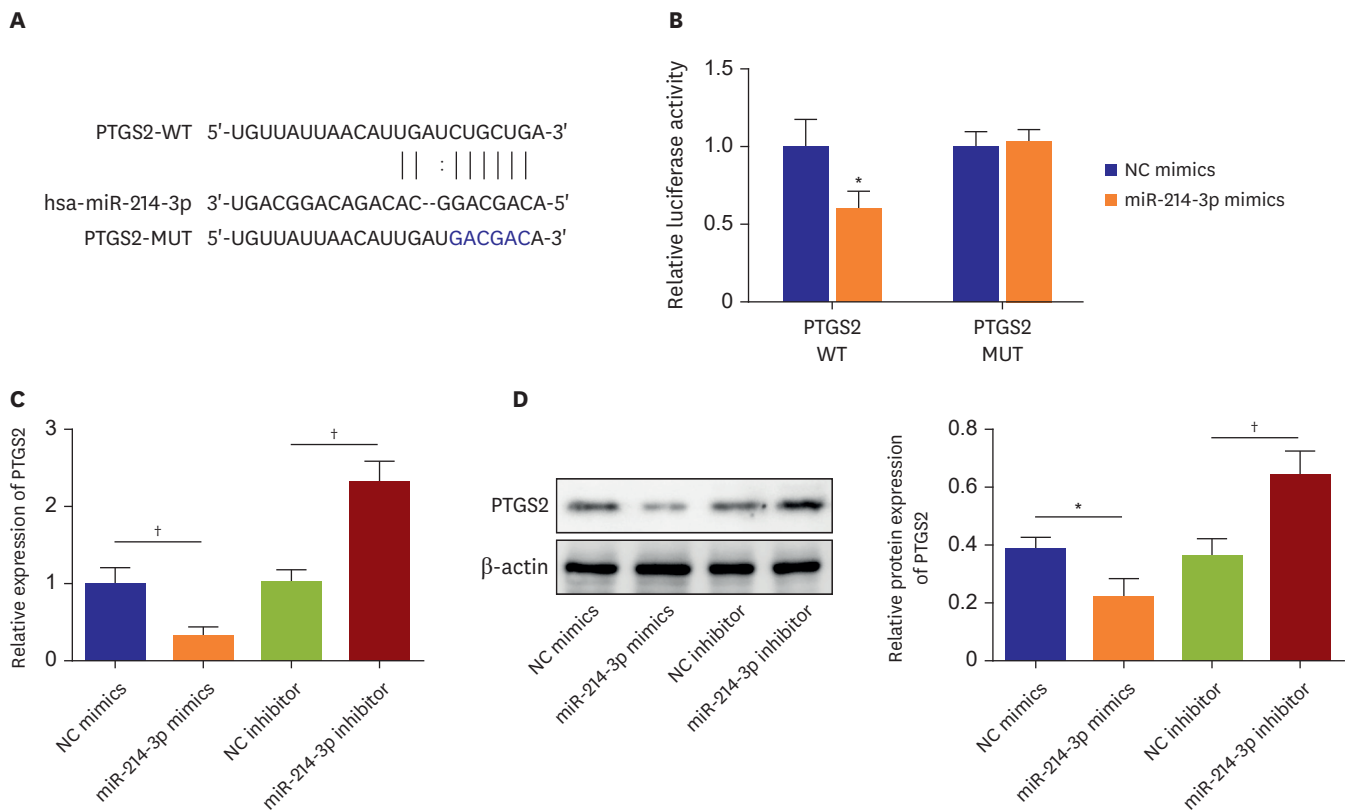

Figure 4. miR-214-3p targeted PTGS2. (A) Starbase 2.0 was used to predict the potential binding site of miR-214-3p and PTGS2. (B) Direct binding of miR-214-3p and CircZNF609 in HCMs was verified by dual luciferase assay. (C) mRNA expression of PTGS2 in HCMs was determined by quantitative polymerase chain reaction. (D) Protein expression of PTGS2 was determined by western blot (n=3).
HCM = human cardiomyocyte; MUT = mutant type; WT = wild-type.
*p<0.05; †p<0.01; ‡p<0.001.

CircZNF609 aggravated H/R induced myocardial injury by targeting miR-214-3p/PTGS2 axis in human cardiomyocytes

Whether miR-214-3p/PTGS2 axis mediated the effect of CircZNF609 in H/R induced myocardial injury was investigated. HCMs was transfected with si-CircZNF609 or co-transfected with si-CircZNF609 and miR-214-3p inhibitor and si-PTGS2, and further exposed to H/R treatment. **Figure 5A** illustrated that knockdown of CircZNF609 restored the proliferation of H/R–treated HCMs ($52.84\pm15.28\%$ vs. $86.49\pm6.33\%$, p=0.024). However, miR-214-3p inhibitor compromised the effect of CircZNF609 knockdown ($86.49\pm6.33\%$ vs. $58.11\pm9.51\%$, p=0.013) while inhibition of PTGS2 by si-PTGS2 further revered the effect on cell proliferation ($58.11\pm9.51\%$ vs. $91.46\pm8.31\%$, p=0.010) (**Figure 5A**). LDH assay revealed that inhibition of CircZNF609 attenuated H/R induced cytotoxicity (2.56 ± 0.24 vs. 1.44 ± 0.20, p=0.003). miR-214-3p inhibitor reversed the inhibitory effect on cell cytotoxicity mediated by CircZNF609 inhibition (1.44 ± 0.20 vs. 2.66 ± 0.11, p=0.001), whereas inhibition of PTGS2 weakened the effect of inhibition of miR-214-3p (2.66 ± 0.11 vs. 1.62 ± 0.36, p=0.009) (**Figure 5B**). Similarly, the repressive role of CircZNF609 on the generation of ROS was diminished by co-inhibition of miR-214-3p, and co-downregulation of PTGS2 remarkably reduced ROS level, reversing the biological role of miR-214-3p inhibitor (**Figure 5C**). Apoptotic detections demonstrated that inhibition of CircZNF609 attenuated H/R–triggered cell apoptosis ($34.40\pm1.80\%$ vs. $19.89\pm2.76\%$, p=0.002), but these effects was abolished by miR-214-3p inhibitor ($19.89\pm2.76\%$ vs. $26.64\pm2.30\%$, p=0.031), however, downregulation of PTGS2 further repressed the apoptosis, diminishing the effect on apoptosis mediated by miR-214-3p inhibitor ($26.64\pm2.30\%$ vs. $17.61\pm3.42\%$, p=0.019) (**Figure 5D and E**). Western blots showed that inhibition of miR-214-3p restrained the promoting effect on Bcl-2 expression (0.75 ± 0.07 vs. 0.44 ± 0.07, p<0.005) and the inhibitory effect on Bax (0.40 ± 0.10 vs. 0.70 ± 0.06, p=0.012) and cleaved caspase 3 (0.30 ± 0.05 vs. 0.56 ± 0.06, p=0.01) levels caused by CircZNF609 silence, whereas these trends were all abolished by co-inhibition of PTGS2 (Bcl-2, 0.44 ± 0.07 vs. 0.63 ± 0.44, p=0.014; Bax, 0.70 ± 0.06 vs. 0.49 ± 0.05, p=0.008; cleaved-caspase 3, 0.56 ± 0.06 vs. 0.41 ± 0.04, p=0.021) (**Figure 5F**). Together, our rescue experiments suggested that CircZNF609 aggravated H/R induced myocardial injury by regulating miR-214-3p/PTGS2 axis.

CircZNF609/miR-214-3p/PTGS2 axis regulated hypoxia/reoxygenation-induced injury in mouse cardiomyocytes and human umbilical vein endothelial cells

Based on previous experimental data, we further validated our main findings in H/R induced mouse cardiomyocytes and HUVECs. In brief, mouse myocardial cells and HUVECs were following divided into five group: control, H/R, H/R+si-CircZNF609, H/R+si-CircZNF609+miR-214-3p inhibitor, H/R+si-CircZNF609+miR-214-3p inhibitor+si-PTGS2. The corresponding transfection efficiency were showed in **Figure 6A**, the expressions of CircZNF609 (cardiomyocytes, 1.00 ± 0.17 vs. 2.31 ± 0.29, p=0.003; HUVECs, 1.00 ± 0.15 vs. 2.02 ± 0.20, p=0.002) and PTGS2 (cardiomyocytes, 1.00 ± 0.22 vs. 3.15 ± 0.39, p=0.001; HUVECs, 1.00 ± 0.19 vs. 2.85 ± 0.41, p=0.002) were obviously increased while miR-214-3p (cardiomyocytes, 1.00 ± 0.10 vs. 0.48 ± 0.12, p=0.005; HUVECs, 1.00 ± 0.06 vs. 0.43 ± 0.22, p=0.011) was downregulated in mouse cardiomyocytes and HUVECs after H/R stimulation. After si-CircZNF609 transfection, CircZNF609 (cardiomyocytes, 2.31 ± 0.29 vs. 1.27 ± 0.18, p=0.006; HUVECs, 2.02 ± 0.20 vs. 1.22 ± 0.26, p=0.014) and PTGS2 (3.15 ± 0.39 vs. 1.80 ± 0.34, p=0.011; 2.85 ± 0.41 vs. 2.00 ± 0.41, p=0.031) were following greatly reduced while miR-214-3p (cardiomyocytes, 0.48 ± 0.12 vs. 0.86 ± 0.07, p=0.003; HUVECs, 0.43 ± 0.22 vs. 0.97 ± 0.12, p=0.020) was elevated, however, co-transfection with miR-214-3p inhibitor remarkably inhibited miR-214-3p level (cardiomyocytes, 0.86 ± 0.07 vs. 0.39 ± 0.10, p=0.003; HUVECs, 0.97 ± 0.12 vs. 0.30 ± 0.16, p=0.004), but restored PTGS2 level (cardiomyocytes,
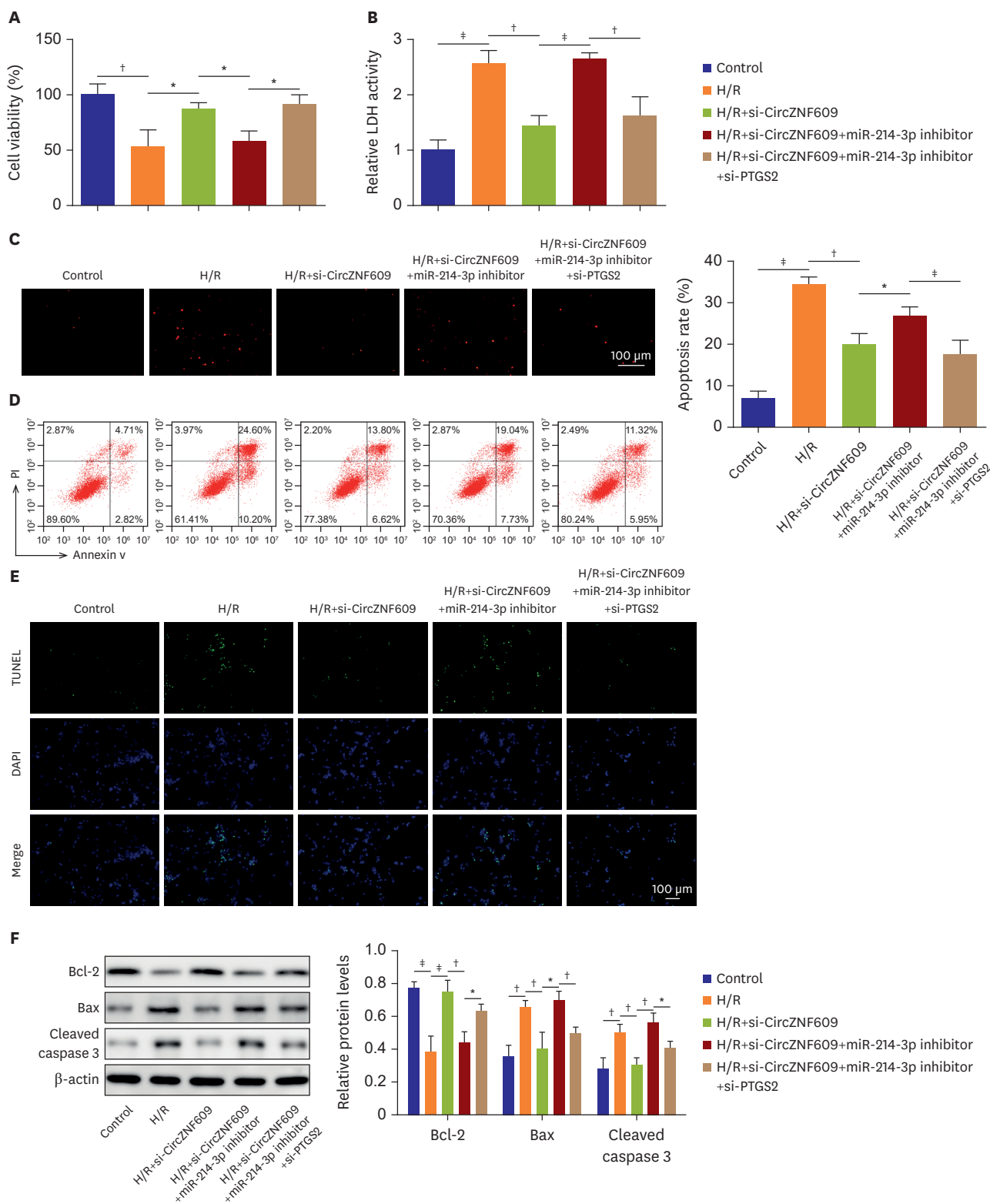
Figure 5. CircZNF609 aggravated H/R induced myocardial injury via regulating miR-214-3p/PTGS2 axis. HCMs were transfected with si-CircZNF609 or co-transfected si-CircZNF609 with miR-214-3p inhibitor and si-PTGS2. Then the cells were subjected to H/R stimulation. (A) Cell proliferation was evaluated by CCK-8 assay. (B) Cytotoxicity was evaluated by LDH assay. (C) ROS generation was detected by a ROS kit. (D) Cell apoptosis was determined by flow cytometry. (E) Cell apoptosis was determined by TUNEL. (F) Protein level of Bcl-2, Bax, cleaved caspase 3 were evaluated by western blots (n = 3).
HCM = human cardiomyocyte; H/R = hypoxia/reoxygenation; LDH = lactate dehydrogenase; ROS = reactive oxygen species.
*p<0.05; †p<0.01; ‡p<0.001.

1.80±0.34 vs. 2.80±0.15, p=0.009; HUVECs, 2.00±0.41 vs. 3.60±0.27, p=0.001) (**Figure 6A**). Importantly, si-PTGS2 transfection decreased PTGS2 expression again (cardiomyocytes, 2.80±0.15 vs. 1.55±0.21, p=0.001; HUVECs, 3.60±0.27 vs. 1.64±0.30, p=0.001) (**Figure 6A**). All of that indicated the corresponding RNAs were successfully transfected. By CCK-8 and LDH detections, we observed that knockdown of CircZNF609 greatly enhanced cell viability (cardiomyocytes, 50.12±8.76% vs. 82.51±7.39%, p=0.008; HUVECs, 49.40±6.61% vs. 93.18±8.60%, p=0.002) and suppressed LDH generation (cardiomyocytes, 2.70±0.30 vs. 1.49±0.23, p=0.005; HUVECs, 2.28±0.16 vs. 1.39±0.34, p=0.016), but miR-214-3p
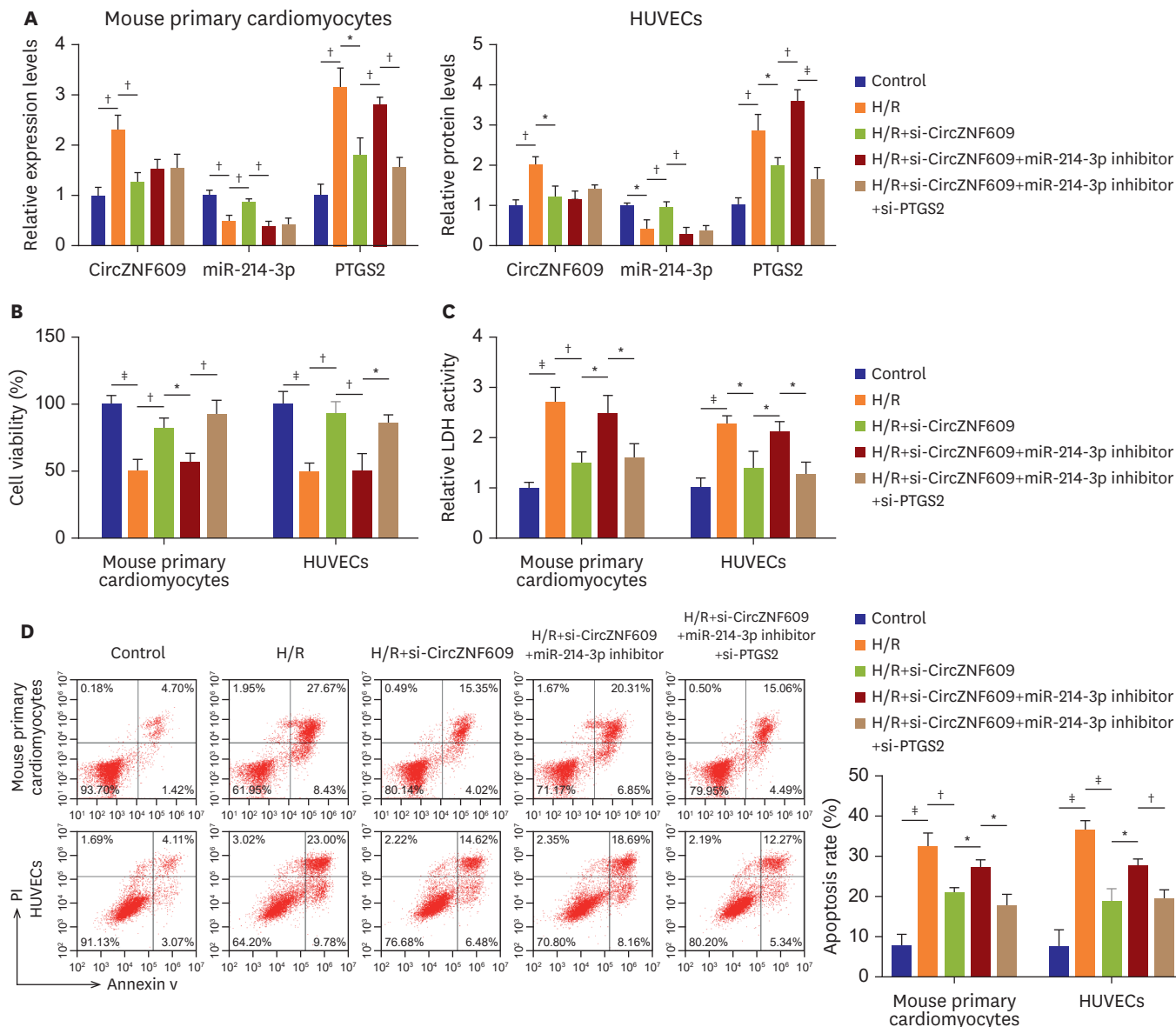

Figure 6. CircZNF609/miR-214-3p/PTGS2 axis regulated H/R-induced injury in mouse myocardial cells and HUVECs. Primary mouse cardiomyocytes and HUVECs were cultured and divided into five group: control, H/R, H/R+si-CircZNF609, H/R+si-CircZNF609+miR-214-3p inhibitor, H/R+si-CircZNF609+miR-214-3p inhibitor+si-PTGS2. (A) The levels of CircZNF609, miR-214-3p and PTGS2 were detected by quantitative polymerase chain reaction. (B) The cell viability was tested by CCK8 assay. (D) The activity of LDH was determined by commercial kit. (E) The cell apoptosis was investigated by flow cytometry. Three independent experiments were performed in each group.
HCM = human cardiomyocyte; H/R = hypoxia/reoxygenation; LDH = lactate dehydrogenase; HUVEC = human umbilical vein endothelial cell.
*p<0.05; †p<0.01; ‡p<0.001.

co-silence partly reduced cell viability (cardiomyocytes, 82.51±7.39% vs. 56.97±6.48%, p=0.011; HUVECs, 93.18±8.60% vs. 50.07±13.18%, p=0.001) and promoted LDH generation (cardiomyocytes, 1.49±0.23 vs. 2.48±0.36, p=0.017; HUVECs, 1.39±0.34 vs. 2.11±0.21, p=0.037) on these basis, partly diminished the biological effects of CircZNF609 downregulation. Moreover, inhibition of PTGS2 strikingly abolished the inhibitory roles of miR-214-3p inhibitor, and further rescued the protective roles of CircZNF609 silence in H/R-triggered damage in cardiomyocytes (cell viability 56.97±6.48% vs. 92.13±10.77%, p=0.008; LDH 2.48±0.36 vs. 1.60±0.28, p=0.030) and HUVECs (cell viability 50.07±13.18% vs. 86.05±5.84%, p=0.013; LDH 2.11±0.21 vs. 1.28±0.24, p=0.011) (**Figure 6B and C**). Similarly, apoptotic assay suggested that knockdown of CircZNF609 greatly reduced H/R-induced cell apoptotic rate (cardiomyocytes, 32.24±3.45% vs. 20.88±1.33%, p=0.006; HUVECs, 36.44±2.35% vs. 18.68±3.17%, p=0.001), and miR-214-3p co-silencing further increased cell apoptosis (cardiomyocytes, 20.88±1.33% vs. 27.06±1.98%, p=0.011; HUVECs, 18.68±3.17% vs. 27.47±1.79%, p=0.014), however, these effects of miR-214-3p inhibitor were reversed by PTGS2 downregulation (cardiomyocytes, 27.06±1.98% vs. 17.43±3.06%, p=0.010; HUVECs, 27.47±1.79% vs. 19.44±2.17%, p=0.008) (**Figure 6D**). Overall, these results further confirmed that protective mechanism of CircZNF609 in H/R-induced myocardial injury by regulating miR-214-3p/PTGS2 signaling.

Knockdown of CircZNF609 alleviated acute myocardial infarction in vivo

To further investigate the function of CircZNF609 in vivo, a MIRI mouse model was established. As shown in **Figure 7A**, the area of myocardial infarction of MIRI mice was significantly decreased by silencing of CircZNF609 (41.27±7.22 vs. 19.40±7.22, p=0.011). Following qPCR assay showed that the levels of CircZNF609 (1.00±0.19 vs. 3.10±0.30, p=0.001) and PTGS2 (1.00±0.28 vs. 2.16±0.18, p=0.004) were significantly increased, while miR-214-3p level (1.00±0.08 vs. 0.43±0.14, p=0.004) was notably decreased in model mice, however, all these trends were partially reversed after si-CircZNF609 transfection (CircZNF609, 2.87±0.42 vs. 1.42±0.29, p=0.008; miR-214-3p, 0.48±0.11 vs. 0.85±0.12, p=0.018; PTGS2, 2.40±0.22 vs. 1.54±0.23, p=0.009) (**Figure 7B, C, and D**). Using TUENL assay, we found that cell apoptotic rate in myocardial tissues of model mice were significantly increased compared to that in sham group mice (10.05±3.09 vs. 63.66±6.9, p=0.000), however, knockdown of CircZNF609 obviously alleviated cell apoptosis (67.68±2.99 vs. 25.21±4.87, p=0.000) (**Figure 7E**). Compared with sham group, Bax (0.23±0.08 vs. 0.76±0.07, p=0.001) and cleaved-caspase 3 (0.21±0.05 vs. 0.71±0.09, p=0.001) were enhanced but Bcl2 level (0.72±0.06 vs. 0.41±0.09, p=0.008) was reduced in model group, however, all these trends were reversed by CircZNF609 downregulation (Bax, 0.70±0.10 vs. 0.38±0.05, p=0.009; cleaved-caspase 3, 0.68±0.13 vs. 0.45±0.06, p=0.005; Bcl2, 0.39±0.05 vs. 0.65±0.08, p=0.008) (**Figure 7F**). Altogether, knockdown of CircZNF609 alleviated MIRI in vivo.

DISCUSSION

MIRI was defined as a complex disease process in which the blood supplement is restored by thrombolysis and interventional therapy after ischemia. Severe MIRI might result in metabolic dysfunction, structural damage, generation of oxygen free radicals and calcium overload, which will cause secondary damage to cardiomyocytes.[3] In present study, we revealed a circRNA, CircZNF609, played critical role in aggravation of MIRI. CircZNF609 promoted apoptosis, generation of ROS and attenuated proliferation of myocytes in H/R model via targeting miR-214-3p/PTGS2 axis. In addition, CircZNF609 was found to alleviate
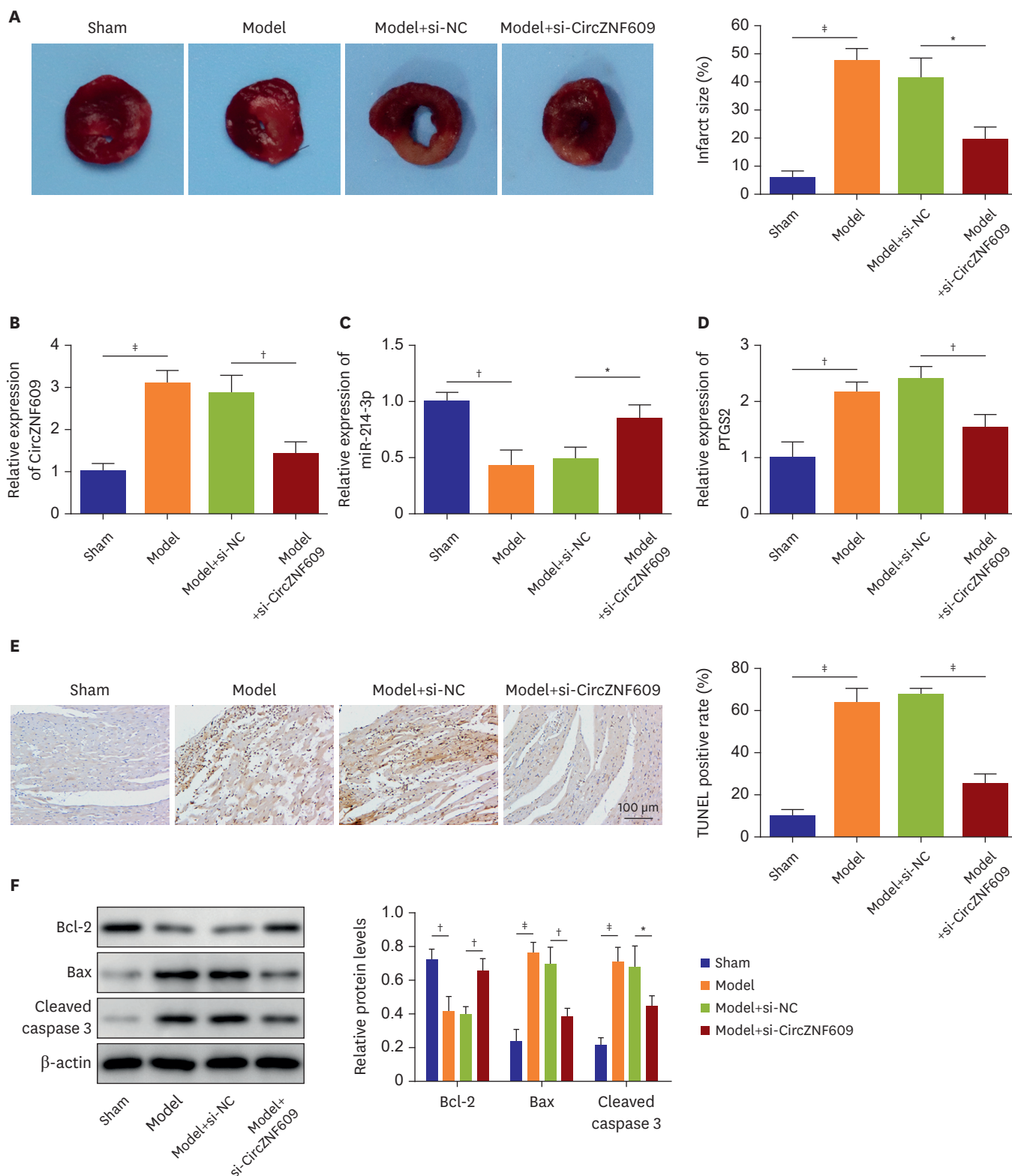
Figure 7. Knockdown of CircZNF609 alleviated MIRI in vivo. (A) The area of myocardial infarction in mice was determined. (B, C, D) The levels of CircZNF609, miR-214-3p and PTGS2 in myocardial tissues of mice were investigated by quantitative polymerase chain reaction. (E) The apoptosis rate was tested by TUNEL staining. (F) The protein levels of Bax, Bcl-2 and cleaved caspase 3 in myocardial tissues of mice were examined by western blot (n=5).
MIRI = myocadiac ischemia reperfusion injury.
*p<0.05; †p<0.01; ‡p<0.001.

the progression of AMI in vivo. Thus, our study firstly explored the function of CircZNF609 in AMI in vitro and in vivo, which supplemented the biological function of CircZNF609.

Recently evidence have revealed that circRNA were involved in the progress of AMI. A study using expressing profiling chips verified that 535 up-regulated circRNA in AMI patients. Some of the dysregulated circRNA regulated multiple signal pathways in the AMI progress. For instance, circRNA CDYL was reported to induces myocardial regeneration after AMI through the miR-4793-5p/APP axis.[16] It was demonstrated that CircMACF1 suppressed AMI injury via targeting miR-500b-5p/EMP1 axis.[23] In terms of MIRI, several circRNA was reported to show detrimental role in the progress of MIRI. Hu has revealed that CircSAMD4A aggravated apoptosis and inflammation in MIRI via targeting miR-138-5p.[24] Another report has illustrated that circular transcript of NCX1 gene mediated the progress of MIRI through miR-133.[5] circRNA TLK1 was also proved to led an aggravation in MIRI through miR-214/RIPK1 axis.[6] In present study, our novel results revealed a detrimental role of CircZNF609 in MIRI. The regulative work of CircZNF609 in MIRI was at least partly dependent on sponging miR-214-3p.

Generally, circRNA can interact with miRNA binding site and act as a sponge of miRNA, thereby removing inhibition of miRNA on downstream target genes and increasing level of downstream target genes. This mechanism was defined as ceRNA network. Previous studies have shown that CircZNF609 might exhibit its function via sponging multiple miRNAs. CircZNF609 was verified to serve as a ceRNA of miR-134-3p to regulate proliferation in glioma.[25] Another study revealed that CircZNF609 facilitated cell growth and migration in breast cancer via targeting miR-145-5p.[26] Moreover, CircZNF609 was also reported to increase migration in gastric cancer via targeting miR-483-3p.[27] Interestingly, some of the targeted miRNAs of CircZNF609 were proved to show functional significance in MIRI or AMI. For instance, it was indicated by Sun et al.[28] that miR-483-3p regulated injury in AMI via suppressing expression of IGF1. Additionally, miR-145-5p was also proved to show regulative work on the inflammatory response in cardiomyocytes ischemia via downregulating CD40.[29] In our study, we revealed that CircZNF609 sponged miR-214-3p to exert the function in MIRI. Combined with these previous studies, we hypothesized that CircZNF609 might play its critical role in MIRI by targeting multiple miRNAs, which need further investigation to verify.

In conclusion, our study revealed that CircZNF609 knockdown could inhibit the progression of AMI in vitro and in vivo. Mechanically, CircZNF609 exhibited this function via targeting miR-214-3p, thus de-repressing the inhibition of PTGS2 and upregulating the expression of PTGS2. Our study might provide novel mechanical understanding for the treatment of MIRI.

ACKNOWLEDGEMENTS

SUPPLEMENTARY MATERIALS

Supplementary Figure 1
The regulatory relationships between circZNF609 and miRNAs. (A) The Starbase 2.0 (http://starbase.sysu.edu.cn/) was used to predict the downstream miRNA of circZNF609. (B) The luciferase activity in cells was tested by dual luciferase assay. (C) The miRNA expressions

of miR-483-3p, miR-378a-3p, miR-204-5p, miR-136-5p and miR-214-3p were investigated by quantitative polymerase chain reaction.

Click here to view

Supplementary Figure 2

The potential targets of miR-214-3p. (A) The downstream mRNAs of miR-214-3p were predicted by Starbase 2.0 (http://starbase.sysu.edu.cn/). (B) The luciferase activities were tested by dual luciferase assay. (C) The mRNA levels of NLRC5, PTGS2, Bax, MAPK1 and PTEN were detected by quantitative polymerase chain reaction.

Click here to view

REFERENCES

1. Xu G, Zhao X, Fu J, Wang X. Resveratrol increase myocardial Nrf2 expression in type 2 diabetic rats and alleviate myocardial ischemia/reperfusion injury (MIRI). *Ann Palliat Med* 2019;8:565-75.
   PUBMED | CROSSREF

2. Yuan L, Dai X, Fu H, et al. Vaspin protects rats against myocardial ischemia/reperfusion injury (MIRI) through the TLR4/NF-κB signaling pathway. *Eur J Pharmacol* 2018;835:132-9.
   PUBMED | CROSSREF

3. Shen Y, Liu X, Shi J, Wu X. Involvement of Nrf2 in myocardial ischemia and reperfusion injury. *Int J Biol Macromol* 2019;125:496-502.
   PUBMED | CROSSREF

4. Zhou LY, Zhai M, Huang Y, et al. The circular RNA ACR attenuates myocardial ischemia/reperfusion injury by suppressing autophagy via modulation of the Pink1/ FAM65B pathway. *Cell Death Differ* 2019;26:1299-315.
   PUBMED | CROSSREF

5. Li M, Ding W, Tariq MA, et al. A circular transcript of *ncx1* gene mediates ischemic myocardial injury by targeting miR-133a-3p. *Theranostics* 2018;8:5855-69.
   PUBMED | CROSSREF

6. Song YF, Zhao L, Wang BC, et al. The circular RNA TLK1 exacerbates myocardial ischemia/reperfusion injury via targeting miR-214/RIPK1 through TNF signaling pathway. *Free Radic Biol Med* 2020;155:69-80.
   PUBMED | CROSSREF

7. Legnini I, Di Timoteo G, Rossi F, et al. Circ-ZNF609 is a circular RNA that can be translated and functions in myogenesis. *Mol Cell* 2017;66:22-37.e9.
   PUBMED | CROSSREF

8. Liu C, Yao MD, Li CP, et al. Silencing of circular RNA-ZNF609 ameliorates vascular endothelial dysfunction. *Theranostics* 2017;7:2863-77.
   PUBMED | CROSSREF

9. Carnieto A Jr, Dourado PM, Luz PL, Chagas AC. Selective cyclooxygenase-2 inhibition protects against myocardial damage in experimental acute ischemia. *Clinics (Sao Paulo)* 2009;64:245-52.
   PUBMED | CROSSREF

10. Salloum FN, Hoke NN, Seropian IM, et al. Parecoxib inhibits apoptosis in acute myocardial infarction due to permanent coronary ligation but not due to ischemia-reperfusion. *J Cardiovasc Pharmacol* 2009;53:495-8.
    PUBMED | CROSSREF

11. Zhao J, Wang F, Zhang Y, et al. Sevoflurane preconditioning attenuates myocardial ischemia/reperfusion injury via caveolin-3-dependent cyclooxygenase-2 inhibition. *Circulation* 2013;128 Suppl 1:S121-9.
    PUBMED | CROSSREF

12. Ruan Z, Wang S, Yu W, Deng F. LncRNA MALAT1 aggravates inflammation response through regulating PTGS2 by targeting miR-26b in myocardial ischemia-reperfusion injury. *Int J Cardiol* 2019;288:122.
    PUBMED | CROSSREF

13. Yang J, Huang X, Hu F, Fu X, Jiang Z, Chen K. LncRNA ANRIL knockdown relieves myocardial cell apoptosis in acute myocardial infarction by regulating IL-33/ST2. *Cell Cycle* 2019;18:3393-403.
    PUBMED | CROSSREF

14. Zhou M, Zou YG, Xue YZ, et al. Long non-coding RNA H19 protects acute myocardial infarction through activating autophagy in mice. *Eur Rev Med Pharmacol Sci* 2018;22:5647-51.
PUBMED

15. Zhang H, Wang J, Du A, Li Y. MiR-483-3p inhibition ameliorates myocardial ischemia/reperfusion injury by targeting the MDM4/p53 pathway. *Mol Immunol* 2020;125:9-14.
PUBMED | CROSSREF

16. Zhao J, Chen F, Ma W, Zhang P. Suppression of long noncoding RNA NEAT1 attenuates hypoxia-induced cardiomyocytes injury by targeting miR-378a-3p. *Gene* 2020;731:144324.
PUBMED | CROSSREF

17. Rong J, Pan H, He J, et al. Long non-coding RNA KCNQ1OT1/microRNA-204-5p/LGALS3 axis regulates myocardial ischemia/reperfusion injury in mice. *Cell Signal* 2020;66:109441.
PUBMED | CROSSREF

18. Lin Y, Dan H, Lu J. Overexpression of microRNA-136-3p alleviates myocardial injury in coronary artery disease via the Rho A/ROCK signaling pathway. *Kidney Blood Press Res* 2020;45:477-96.
PUBMED | CROSSREF

19. Yang K, Shi J, Hu Z, Hu X. The deficiency of miR-214-3p exacerbates cardiac fibrosis via miR-214-3p/NLRC5 axis. *Clin Sci (Lond)* 2019;133:1845-56.
PUBMED | CROSSREF

20. Bai M, Pan CL, Jiang GX, Zhang YM, Zhang Z. CircHIPK3 aggravates myocardial ischemia-reperfusion injury by binding to miRNA-124-3p. *Eur Rev Med Pharmacol Sci* 2019;23:10107-14.
PUBMED

21. Liu K, Wang F, Wang S, Li WN, Ye Q. Mangiferin attenuates myocardial ischemia-reperfusion injury via MAPK/Nrf-2/HO-1/NF-κB in vitro and in vivo. *Oxid Med Cell Longev* 2019;2019:7285434.
PUBMED | CROSSREF

22. Xing X, Guo S, Zhang G, et al. miR-26a-5p protects against myocardial ischemia/reperfusion injury by regulating the PTEN/PI3K/AKT signaling pathway. *Braz J Med Biol Res* 2020;53:e9106.
PUBMED | CROSSREF

23. Zhao B, Li G, Peng J, et al. CircMACF1 attenuates acute myocardial infarction through miR-500b-5p-EMP1 axis. *J Cardiovasc Transl Res* 2021;14:161-72.
PUBMED | CROSSREF

24. Hu X, Ma R, Cao J, Du X, Cai X, Fan Y. CircSAMD4A aggravates H/R-induced cardiomyocyte apoptosis and inflammatory response by sponging miR-138-5p. *J Cell Mol Med* 2022;26:1776-84.
PUBMED | CROSSREF

25. Tong H, Zhao K, Wang J, Xu H, Xiao J. CircZNF609/miR-134-5p/BTG-2 axis regulates proliferation and migration of glioma cell. *J Pharm Pharmacol* 2020;72:68-75.
PUBMED | CROSSREF

26. Wang S, Xue X, Wang R, et al. CircZNF609 promotes breast cancer cell growth, migration, and invasion by elevating p70S6K1 via sponging miR-145-5p. *Cancer Manag Res* 2018;10:3881-90.
PUBMED | CROSSREF

27. Wu W, Wei N, Shao G, Jiang C, Zhang S, Wang L. circZNF609 promotes the proliferation and migration of gastric cancer by sponging miR-483-3p and regulating CDK6. *Onco Targets Ther* 2019;12:8197-205.
PUBMED | CROSSREF

28. Sun H, Cai J, Xu L, et al. miR-483-3p regulates acute myocardial infarction by transcriptionally repressing insulin growth factor 1 expression. *Mol Med Rep* 2018;17:4785-90.
PUBMED | CROSSREF

29. Yuan M, Zhang L, You F, et al. MiR-145-5p regulates hypoxia-induced inflammatory response and apoptosis in cardiomyocytes by targeting CD40. *Mol Cell Biochem* 2017;431:123-31.
PUBMED | CROSSREF